Genome-wide RNA interference screening reveals a COPI-MAP2K3 pathway required for YAP regulation

Yong Joon Kim[a,b,1], Eunji Jung[a,1], Eunbie Shin[a], Sin-Hyoung Hong[c,d], Hui Su Jeong[e], Gayeong Hur[a,f], Hye Yun Jeong[a], Seung-Hyo Lee[a], Ji Eun Lee[e,g,2], Gun-Hwa Kim[c,d,2], and Joon Kim[a,2]

[a]Graduate School of Medical Science and Engineering, Korea Advanced Institute of Science and Technology, 34141 Daejeon, Korea; [b]Department of Ophthalmology, Institute of Vision Research, Severance Hospital, Yonsei University College of Medicine, 06273 Seoul, Korea; [c]Drug & Disease Target Team, Division of Bioconvergence Analysis, Korea Basic Science Institute, 28119 Cheongju, Korea; [d]Department of Bio-Analytical Science, University of Science and Technology, 34113 Daejeon, Korea; [e]Department of Health Sciences and Technology, Samsung Advanced Institute for Health Sciences & Technology, Sungkyunkwan University, 06355 Seoul, Korea; [f]R&D Division, GenoFocus Inc., 34014 Daejeon, Korea; and [g]Samsung Biomedical Research Institute, Samsung Medical Center, 06351 Seoul, Korea

Edited by Akira Suzuki, Medical Institute of Bioregulation, Kyushu University, Fukuoka, Japan, and accepted by Editorial Board Member Tak W. Mak July 9, 2020 (received for review September 4, 2019)

The transcriptional regulator YAP, which plays important roles in the development, regeneration, and tumorigenesis, is activated when released from inhibition by the Hippo kinase cascade. The regulatory mechanism of YAP in Hippo-low contexts is poorly understood. Here, we performed a genome-wide RNA interference screen to identify genes whose loss of function in a Hippo-null background affects YAP activity. We discovered that the coatomer protein complex I (COPI) is required for YAP nuclear enrichment and that COPI dependency of YAP confers an intrinsic vulnerability to COPI disruption in YAP-driven cancer cells. We identified MAP2K3 as a YAP regulator involved in inhibitory YAP phosphorylation induced by COPI subunit depletion. The endoplasmic reticulum stress response pathway activated by COPI malfunction appears to connect COPI and MAP2K3. In addition, we provide evidence that YAP inhibition by COPI disruption may contribute to transcriptional up-regulation of PTGS2 and proinflammatory cytokines. Our study offers a resource for investigating Hippo-independent YAP regulation as a therapeutic target for cancers and suggests a link between YAP and COPI-associated inflammatory diseases.

Hippo-YAP pathway | RNAi screen | coatomer

YAP and its paralog TAZ are transcriptional coactivators that drive high levels of transcriptional outputs, promoting cell proliferation and survival (1, 2). YAP and TAZ also function as transcriptional corepressors that control a number of targets including tumor suppressor genes (3, 4). The Hippo kinase cascade is a central regulator of YAP/TAZ activity (5, 6). Phosphorylation of YAP/TAZ by the Hippo core components LATS1 and LATS2 causes cytoplasmic sequestration and proteasomal degradation of YAP/TAZ (7). Various upstream regulatory inputs associated with cell junctions and the actin cytoskeleton control YAP/TAZ activity mainly through their influence on the Hippo kinases (1, 8). Some regulatory components, including AMOT, AMPK, and AKT, have been shown to modulate YAP/TAZ activity in a Hippo-independent manner (9–11). Hippo-independent regulatory inputs are usually masked in the context of high Hippo signaling activities. When Hippo signaling attenuates, the presence of Hippo-independent regulation of YAP/TAZ becomes clear.

YAP and TAZ are involved in multiple aspects of the cancer phenotype, such as tumorigenesis, tumor stem-like property, anticancer drug resistance, metastasis, and immune evasion (12, 13). Higher levels of YAP/TAZ expression and nuclear enrichment have been detected in various types of human cancers (14, 15). Although YAP/TAZ gene amplifications were identified in head and neck squamous cell carcinomas (14), genetic or epigenetic silencing of the Hippo signaling components might be a more frequent cause of YAP/TAZ hyperactivation in cancer. Thus, Hippo-independent regulatory components can play an important role in determining YAP/TAZ activity in cancer cells and may serve as suitable drug targets for suppressing YAP-driven cancer phenotype. Currently, our understanding of the Hippo-independent regulation of YAP/TAZ is incomplete in part because there is no comprehensive list of genes involved in the regulation.

Here, we systematically investigate Hippo-independent YAP/TAZ regulation using genome-wide RNA interference (RNAi) phenotypic screens. We identify a number of genes that can be classified as positive or negative factors of YAP expression or nuclear enrichment. Among the candidates we focused on were COPI subunits whose knockdown resulted in cytoplasmic sequestration of YAP in a Hippo-null context. We found that suppression of the expression of the COPI subunits ARCN1 and COPA causes inhibitory phosphorylation of YAP at Ser127 by MAP2K3. Consistent with the fact that COPA germline mutations cause an inflammatory genetic disorder called COPA syndrome (16), we found that depletion of either COPA or YAP causes up-regulation of proinflammatory cytokines. Our data will be valuable for gaining a deeper insight into the multilayered YAP regulatory network.

Results

Identification of Hippo-Independent Regulators of YAP Activity. To identify components of Hippo-independent YAP regulations, we

Significance

YAP is a transcriptional regulator governing gene expression programs underlying cell proliferation and survival. In addition, YAP has been highlighted as a key player in various stages of cancer pathogenesis. Currently, our understanding of the regulation of YAP activity is incomplete in part because there is no comprehensive list of genes related to the regulation. In this paper, we report the result of a genome-wide RNA interference screen to identify genes whose loss of function affects the activity of YAP. We discovered a number of genes that can be classified as positive or negative factors of YAP stability or nuclear enrichment. Our data will be valuable for gaining a deeper insight into complex YAP regulation.

Author contributions: Y.J.K., E.J., S.-H.L., J.E.L., and J.K. designed research; Y.J.K., E.J., E.S., S.-H.H., H.S.J., G.H., H.Y.J., and G.-H.K. performed research; G.-H.K. contributed new reagents/analytic tools; Y.J.K., E.J., H.S.J., S.-H.L., J.E.L., G.-H.K., and J.K. analyzed data; and Y.J.K., E.J., J.E.L., G.-H.K., and J.K. wrote the paper.

The authors declare no competing interest.

This article is a PNAS Direct Submission. A.S. is a guest editor invited by the Editorial Board.

[1]Y.J.K. and E.J. contributed equally to this work.

[2]To whom correspondence may be addressed. Email: jieun.lee@skku.edu, genekgh@kbsi.re.kr, or joonkim@kaist.ac.kr.

This article contains supporting information online at https://www.pnas.org/lookup/suppl/doi:10.1073/pnas.1915387117/-/DCSupplemental.

First published August 3, 2020.

performed an image-based genome-wide RNAi screen. First, we generated hTERT-immortalized retinal pigmented epithelial cells carrying null mutations in LATS1 and LATS2 genes (RPE1-LATS1/2 DKO) using the CRISPR/Cas9 system (17). Frameshift mutations in the LATS1/2 genes were demonstrated by Sanger sequencing, and reduction of YAP phosphorylation at Ser127 was detected by immunoblot analysis (*SI Appendix*, Fig. S1 *A* and *B*). As expected, conditions known to inhibit YAP, such as confluency, serum starvation, cytochalasin D, and cerivastatin (6, 18, 19), failed to induce cytoplasmic sequestration of YAP in RPE1-LATS1/2 DKO cells (*SI Appendix*, Fig. S1 *C–F*). Nuclear enrichment of YAP was diminished when cell density exceeded confluency even in LATS1/2 DKO cells, suggesting that density-mediated YAP regulation can occur in a Hippo-independent manner. Using RPE1-LATS1/2 DKO cells, we screened a small interfering RNA (siRNA) library targeting 18,055 genes across the human genome (Fig. 1*A*). Automated imaging and an image analysis system provided measurements of the levels of anti-YAP/TAZ immunofluorescence in the nucleus and the perinuclear cytoplasm (Fig. 1*B* and Dataset S1). Data from genes that are not actively expressed (RNA sequencing fragments-per-kilobase-per-million-mapped-reads value of less than 2) in RPE1-LATS1/2 DKO cells were filtered to reduce false positives.

The screen identified multiple genes whose knockdown caused elevation or reduction of nuclear YAP-staining intensities (cutoff values = 3 SDs away from the mean; Fig. 1*C*). We also identified a number of genes that are required for keeping a low cytoplasm/nuclear (c/n) ratio of YAP staining (Fig. 1*D*). There were only a few genes whose knockdown further decreased the YAP c/n ratio, probably because YAP is already enriched in the nucleus in LATS1/2 DKO cells (Fig. 1*D*). Functional annotation and bioinformatics analysis indicated that the ubiquitin-proteasome pathway and the intracellular membrane-trafficking pathway involving COPI are key determinants of YAP activity in the Hippo-null context (Fig. 1 *E* and *F*). Although the genes encoding the TEAD family, the major binding partners of YAP (20), were not identified as screen hits, several transcriptional regulators that influenced YAP expression or localization were discovered. Knockdown of only three genes (CDC42EP3, NUMA1, and SERPINB8) affected both nuclear YAP intensity and YAP c/n ratio, suggesting that YAP expression/stability control is independent of YAP nuclear translocation control in the Hippo-null context.

COPI Subunit Depletion Reduces YAP Nuclear Localization and Activity. The COPI is a carrier complex that is required for Golgi-to-endoplasmic reticulum (ER) retrograde transport (21). Five subunits among the seven subunits of the COPI complex were identified as screen hits (Fig. 1*D*). Knockdown of *ARCN1* and *COPA* showed greater increases in the YAP c/n ratio than other subunits and thus was selected for further analysis. Two independent siRNAs for ARCN1 and COPA significantly increased the proportion of cells exhibiting equivalent YAP immunoreactivity levels in the nucleus and the cytoplasm (Fig. 2 *A* and *B*). Depletion of ARCN1 or COPA in RPE1 LATS1/2 wild-type (WT) cells causes not only cytoplasmic sequestration but also nuclear exclusion of YAP, suggesting that basal LATS activity and COPI subunit depletion exert an additive effect on YAP localization (Fig. 2 *C* and *D*). The expression of CTGF, a transcriptional target of YAP, decreased upon *ARCN1* or *COPA* knockdown in both LATS1/2 DKO and WT cells (Fig. 2 *E* and *F*). The TEAD reporter activity was also significantly decreased by ARCN1 and COPA knockdown (Fig. 2*G*). We next examined changes in the gene expression profile of ARCN1-depleted RPE1-LATS1/2 WT cells using a microarray analysis (Dataset S2). Gene set enrichment analysis (GSEA) of the microarray data revealed a significant reduction of the expression of YAP signature genes (Fig. 2 *H* and *I*). To further demonstrate the association between COPI and YAP, we analyzed the breast cancer cell line MCF7. Depletion of ARCN1 and COPA resulted in cytoplasmic retention of YAP in both LATS1/2 DKO and WT MCF7 cells (*SI Appendix*, Fig. S2 *A–F*). Similar to RPE1 cells, LATS1/2 WT cells showed a higher proportion of cells exhibiting cytoplasmic YAP retention. ARCN1 and COPA knockdown also decreased TEAD reporter activity (*SI Appendix*, Fig. S2*G*). Taken together, these results indicate that intact COPI is required for maintaining nuclear enrichment of YAP.

To find in vivo evidence of the link between COPI and YAP regulation, we examined the effect of COPI subunit knockdown on YAP protein in zebrafish. Both the COPI system and the Hippo-YAP pathway are evolutionarily well conserved. The amino acid sequences of human and zebrafish COPA and YAP show 86.6 and 79.8% identity, respectively. Structural similarity suggests that the zebrafish Yap protein undergoes a similar phosphorylation as in human YAP Ser127 (*SI Appendix*, Fig. S3*A*). To disrupt the expression of *copa*, splicing blocking the morpholino oligonucleotide (MO) was injected into zebrafish eggs. MO-mediated disruption of *copa* transcript splicing was verified by RT-PCR analysis (*SI Appendix*, Fig. S3*B*). MO-mediated knockdown of *copa* resulted in an increase in phosphorylated Yap recognized by anti–phospho-YAP Ser127 antibody (*SI Appendix*, Fig. S3*C*). A previous study showed that zebrafish Yap and Taz are expressed in the retinal pigmented epithelium and the mesenchymal condensations surrounding the retina (22). We observed cytoplasmic sequestration of YAP in cells surrounding the retina (*SI Appendix*, Fig. S3*D*). These results support the idea that COPI defects can cause YAP inactivation.

COPI Subunit Depletion Reduces YAP Dependency in Cancer Cells. We tested whether YAP-dependent cancer cells show a high dependence on intact COPI function for survival. Previously, we demonstrated that the melanoma cell line SKMEL28 does not depend on YAP/TAZ for survival, but SKMEL28 cells that acquired vemurafenib resistance exhibit higher YAP activity and dependency for survival (23). Depletion of ARCN1 or COPA significantly reduced the number of viable cells among vemurafenib-resistant SKMEL28 cells compared to vemurafenib-sensitive (parental) SKMEL28 cells (Fig. 3*A*). In addition, similar to YAP/TAZ double knockdown, ARCN1 and COPA knockdown in vemurafenib-resistant SKMEL28 cells reduced the levels of EGFR and c-MYC (Fig. 3*B*). We also tested other cancer cell lines that require YAP/TAZ activity for survival. Uveal melanoma (92.1), mesothelioma (MSTO-211H), and non–small-cell lung cancer (A549) cell lines exhibited YAP dependency, whereas the survival of ocular choroidal melanoma (OCM1) and MCF7 was not affected by YAP/TAZ knockdown (Fig. 3*C*). According to public genomics data, the YAP-dependent cell lines harbor mutations which can increase YAP activity: *GNAQ* for 92.1, *LATS2* for MSTO-211H, *NF2* for H2373, and *LKB1* for A549. In YAP/TAZ-dependent cancer cell cultures, the number of viable cells significantly reduced in response to ARCN1 or COPA depletion (Fig. 3*D*). Induction of cleaved caspase 3 expression indicated apoptotic cell death in cells depleted of ARCN1 or COPA (Fig. 3*E*). These results suggest that the COPI-YAP connection provides a potential drug target for inhibition of YAP addiction.

MAP2K3 May Mediate YAP Ser127 Phosphorylation and Cytoplasmic Sequestration. YAP phosphorylation by LATS1/2 at Ser127 is the major mechanism of YAP cytoplasmic sequestration, and Ser94 phosphorylation disrupts the YAP-TEAD interaction (1, 9). We found an increase in the level of YAP Ser127 phosphorylation after knockdown of ARCN1 or COPA in both RPE1-LATS1/2 DKO and MCF7-LATS1/2 DKO cells (Fig. 4*A* and *SI Appendix*, Fig. S4*A*). YAP Ser127 phosphorylation levels in RPE1-LATS1/2 DKO cells depleted of ARCN1 or COPA were not as high as in RPE1-LATS1/2 WT cells transfected with control siRNA. An

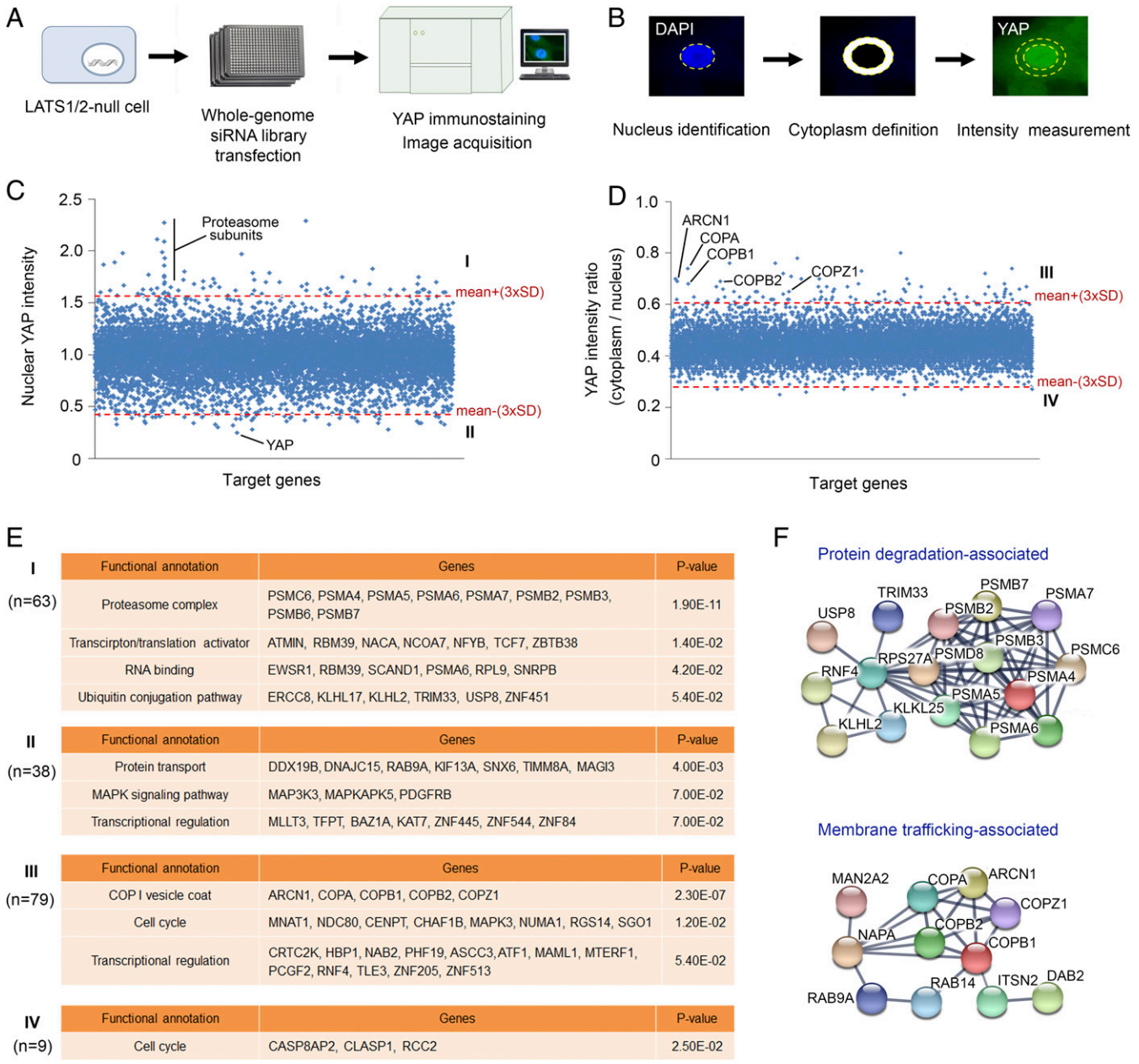

E

	Functional annotation	Genes	P-value
I (n=63)	Proteasome complex	PSMC6, PSMA4, PSMA5, PSMA6, PSMA7, PSMB2, PSMB3, PSMB6, PSMB7	1.90E-11
	Transcirpton/translation activator	ATMIN, RBM39, NACA, NCOA7, NFYB, TCF7, ZBTB38	1.40E-02
	RNA binding	EWSR1, RBM39, SCAND1, PSMA6, RPL9, SNRPB	4.20E-02
	Ubiquitin conjugation pathway	ERCC8, KLHL17, KLHL2, TRIM33, USP8, ZNF451	5.40E-02
II (n=38)	Protein transport	DDX19B, DNAJC15, RAB9A, KIF13A, SNX6, TIMM8A, MAGI3	4.00E-03
	MAPK signaling pathway	MAP3K3, MAPKAPK5, PDGFRB	7.00E-02
	Transcriptional regulation	MLLT3, TFPT, BAZ1A, KAT7, ZNF445, ZNF544, ZNF84	7.00E-02
III (n=79)	COP I vesicle coat	ARCN1, COPA, COPB1, COPB2, COPZ1	2.30E-07
	Cell cycle	MNAT1, NDC80, CENPT, CHAF1B, MAPK3, NUMA1, RGS14, SGO1	1.20E-02
	Transcriptional regulation	CRTC2K, HBP1, NAB2, PHF19, ASCC3, ATF1, MAML1, MTERF1, PCGF2, RNF4, TLE3, ZNF205, ZNF513	5.40E-02
IV (n=9)	Cell cycle	CASP8AP2, CLASP1, RCC2	2.50E-02

F

Fig. 1. RNAi screening identifies Hippo-independent YAP regulators. (*A*) Schematic illustration of a genome-wide siRNA library screen to identify Hippo-independent YAP regulators. (*B*) Automated image analysis for quantification of nuclear and cytoplasmic YAP immunofluorescence intensities. (*C*) A graph showing the result of siRNA library screening. Nuclear YAP intensities in RPE1-LATS1/2 DKO cells were measured. Diamonds represent mean nuclear YAP intensity after knockdown of each gene. (*D*) A graph showing mean values of the cytoplasmic/nuclear ratio of YAP intensity. Four groups of screen hits (I to IV) were defined using three SDs as cutoff values. (*E*) A list of gene ontology enrichments found in each hit group. (*F*) Two clusters of associated hits identified by an analysis of known physical or functional associations between all hits of the four screen hit groups.

increase in YAP phosphorylation at Ser94 was also detected in RPE1-LATS1/2 DKO cells (Fig. 4*A*). These observations suggest that, although not as potent as LATS1/2, there are kinases that mediate YAP phosphorylation in response to COPI subunit depletion. YAP phosphorylation at Ser127 and Ser94 slightly increased in RPE1-LATS1/2 WT cells after ARCN1 or COPA knockdown (Fig. 4*A*). Because no significant increase in activating phosphorylation of LATS1 was observed, it is unlikely that an increase in LATS activity promoted YAP phosphorylation after COPI subunit knockdown in LATS WT cells (*SI Appendix*, Fig. S4*B*). The amount of total YAP protein did not change notably after ARCN1 or COPA knockdown, whereas total TAZ levels consistently decreased (Fig. 4*A*). To demonstrate that YAP phosphorylation is the main cause of YAP cytoplasmic retention after ARCN1 or COPA knockdown, we established RPE1 cells stably expressing YAP-5SA, in which serine residues in all five LATS consensus motifs were mutated to alanine (24). YAP-5SA mutants were primarily localized to the nucleus, regardless of COPI subunit depletion (*SI Appendix*, Fig. S4 *C* and *D*). However, COPA depletion caused a small but statistically significant increase in the number of cells with equivalent YAP distribution in the nucleus and cytoplasm (*SI Appendix*, Fig. S4*D*). This result indicates that COPI defects induce inhibitory YAP phosphorylation but may also promote YAP inhibition through other mechanisms.

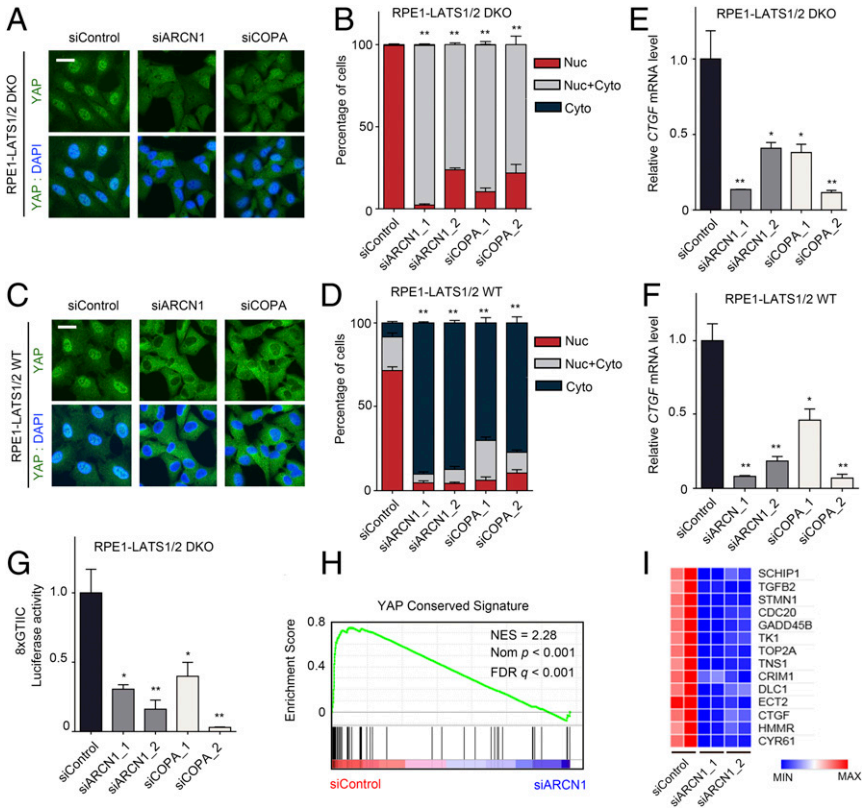

Fig. 2. COPI subunit depletion leads to a decrease in YAP activity through cytoplasmic retention. (*A*) Immunofluorescence micrographs showing YAP localization in RPE1-LATS1/2 DKO cells transfected with the indicated siRNAs for 48 h. (*B*) Quantification of the experiment presented in *A*. Nuc, nuclear YAP enrichment; Nuc+Cyto, equivalent YAP distribution in the nucleus and cytoplasm; and Cyto, cytoplasmic YAP retention. (*C*) Immunofluorescence micrographs showing YAP localization in RPE1-LATS1/2 WT cells. (*D*) Quantification of the experiment presented in *C*. (*E*) qRT-PCR analysis of the expression of the YAP target gene *CTGF* in RPE1-LATS1/2 DKO cells after transfection with the indicated siRNAs for 48 h. (*F*) qRT-PCR analysis of the expression of *CTGF* in RPE1-LATS1/2 WT cells. (*G*) Luciferase reporter assay for YAP transcriptional activity measurement. RPE1-LATS1/2 DKO cells were transfected with the indicated siRNAs for 24 h and then transfected with the 8xGTIIC reporter vector for 24 h before the analysis. (*H*) GSEA of microarray data demonstrating a down-regulation of YAP signature genes in ARCN1-depleted RPE1-LATS1/2 WT cells. (*I*) A heatmap of down-regulated YAP signature genes in ARCN1-depleted RPE1-LATS1/2 WT cells. (Scale bars: 20 μm [*A* and *C*].) (*B* and *D*–*G*) Error bars represent SEM; $n = 3$ independent experiments. $^*P < 0.05$ and $^{**}P < 0.01$ (*t* test).

Next, we employed a kinome-wide RNAi library screen to identify the kinase responsible for YAP phosphorylation in LATS1/2-null cells (Dataset S3). We found several candidate kinases whose knockdown in RPE1-LATS1/2 DKO cells suppressed the YAP cytoplasmic sequestration due to cotransfected ARCN1 siRNA (Fig. 4*B*). MAP2K3 showed the strongest effects on the suppression of the ARCN1 knockdown phenotype and thus was selected for further study. NDR2, which is already known to phosphorylate YAP (25), was also identified by the screen. Cotransfection of MAP2K3 siRNA with ARCN1 or COPA siRNA resulted in a recovery of YAP nuclear enrichment in RPE1-LATS1/2 DKO cells (Fig. 4 *C* and *D*). In addition, depletion of MAP2K3 suppressed YAP phosphorylation at Ser127 induced by ARCN1 or COPA knockdown in LATS1/2 DKO cells (Fig. 4*E*). Small increases in YAP Ser127 phosphorylation in RPE1-LATS1/2 WT and MCF7-LATS1/2 DKO cells after ARCN1 or COPA knockdown was also reversed by cotransfection with MAP2K3 siRNAs (*SI Appendix*, Fig. S5 *A* and *B*). YAP was coimmunoprecipitated with endogenous MAP2K3 (Fig. 4*F*). An in vitro kinase assay showed that MAP2K3 can directly phosphorylate YAP at Ser127 (Fig. 4*G*). Moreover, overexpression of exogenous MAP2K3 increased phosphorylation of YAP as well as its known target P38 MAPK (*SI Appendix*, Fig. S5*C*). Reduction of YAP Ser127 phosphorylation after MAP2K3 knockdown was partially rescued by expression of siRNA-insensitive FLAG-MAP2K3 (*SI Appendix*, Fig. S5*D*). ACRN1 or COPA knockdown caused a YAP protein mobility shift in a gel containing phos-tag acrylamide, and the shift was blocked by MAP2K3 coknockdown (*SI Appendix*, Fig. S5*E*). YAP Ser94 phosphorylation was not clearly reduced by MAP2K3 coknockdown (Fig. 4*E*). Phosphorylation at YAP Ser397, a LATS target site mediating YAP degradation, was not affected by COPI or MAP2K3 knockdown (*SI Appendix*, Fig. S5*F*). These results together suggest that MAP2K3 is involved in YAP inactivation in response to COPI function disturbances. However, MAP2K3 does not appear to phosphorylate all LATS target sites.

TAZ Ser89 phosphorylation was increased by ARCN1 or COPA depletion, and the increase was suppressed by MAP2K3 coknockdown (*SI Appendix*, Fig. S5*E*). However, the reduction of total TAZ levels was not rescued by MAP2K3 coknockdown (Fig. 4*E* and *SI Appendix*, Fig. S5*A*). In addition, a TAZ protein mobility shift was still observed in a phos-tag gel after MAP2K3 coknockdown (*SI Appendix*, Fig. S5*E*). It is likely that COPI subunit depletion results in activation of multiple kinases, including MAP2K3, which recognize TAZ.

NDR kinases, close homologs of LATS1/2, phosphorylate YAP at Ser127 (25). We examined the relative contribution of MAP2K3 and NDR kinases to YAP phosphorylation in LATS1/2 DKO and WT cells. Coknockdown of NDR2 with ARCN1 or COPA in RPE1-LATS1/2 DKO cells resulted in a reduction of YAP Ser127 phosphorylation, whereas the effect of NDR1

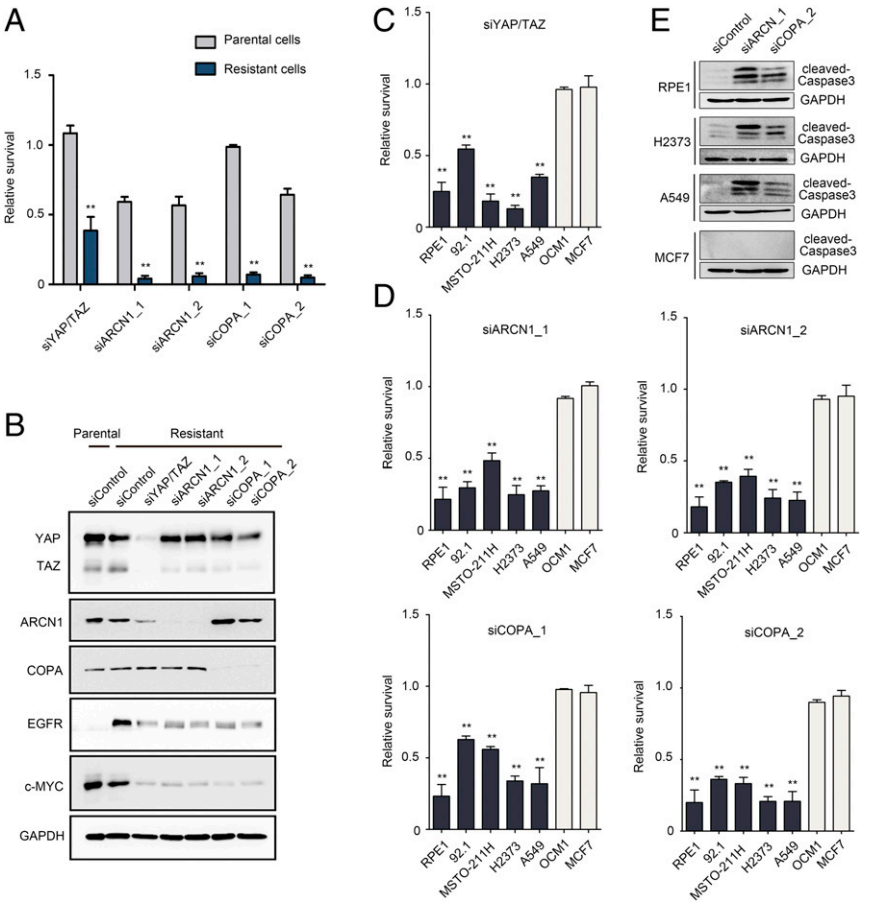

Fig. 3. COPI subunit depletion decreases the viability of cancer cells that exhibit YAP dependency. (*A*) A graph showing relative survival of parental and vemurafenib-resistant SKMEL28 cells after transfection with the indicated siRNAs. Viable cells were quantified using Cell Counting Kit-8. Viability of parental and resistant cells transfected with control siRNA was set to 1. (*B*) Immunoblot analysis of the indicated proteins. Lysates of parental and vemurafenib-resistant SKMEL28 cells transfected with the indicated siRNAs were analyzed. (*C* and *D*). Viable cells were quantified using Cell Counting Kit-8 after transfection with the indicated siRNAs. Viability of each cell type transfected with control siRNA was set to 1. (*E*) Immunoblot analysis of cleaved Caspase 3 expression. (*A*, *C* and *D*) Error bars represent SEM; $n = 3$ independent experiments. $^{**}P < 0.01$ (*t* test).

coknockdown was less obvious (*SI Appendix*, Fig. S6*A*). Comparison between MAP2K3 and NDR1/2 knockdown suggested that MAP2K3 is a major kinase that is responsible for YAP phosphorylation in LATS1/2 DKO background (*SI Appendix*, Fig. S6*B*). We next tested whether MAP2K3 and NDR1/2 contribute to YAP Ser127 phosphorylation in the absence of COPI defects. Depletion of MAP2K3 and NDR1/2 did not noticeably change YAP Ser127 phosphorylation in RPE1 LATS1/2 WT cells, confirming dominant activity of LATS1/2 in YAP phosphorylation (*SI Appendix*, Fig. S6*C*). In RPE1 LATS1/2 DKO cells, depletion of MAP2K3 and NDR1/2 decreased YAP Ser127 phosphorylation (*SI Appendix*, Fig. S6*C*). YAP phosphorylation levels were reduced by MAP2K3 knockdown in MCF7-LATS1/2 WT cells as well as in MCF7-LATS1/2 DKO cells (*SI Appendix*, Fig. S6*C*). Together with the small reduction of YAP Ser127 phosphorylation in MCF7-LATS1/2 null cells (*SI Appendix*, Fig. S2*B*), this suggests that LATS1/2 are not the dominant regulators of YAP in MCF7 cells. In line with this idea, MCF cells were less sensitive to the stimulations that modulate the activities of the core Hippo kinases, such as confluency, serum starvation, and actin disassembly (*SI Appendix*, Fig. S6 *D* and *E*). However, sensitivity of MCF7 cells to cerevastatin treatment, which affects YAP activity through RHO-GTPase, was LATS1/2 dependent (*SI Appendix*, Fig. S6 *D* and *E*).

Depletion of COPA did not affect nuclear YAP accumulation in HEK293A LATS1/2 DKO cells, whereas COPA knockdown resulted in cytoplasmic sequestration of YAP in HEK293A LATS1/2 WT cells (*SI Appendix*, Fig. S7*A*). Unexpectedly, YAP Ser127 phosphorylation did not noticeably increase after COPA knockdown in HEK293A LATS1/2 WT and DKO cells (*SI Appendix*, Fig. S7*B*). We speculate that Hippo-independent COPI malfunction signal alone can inhibit YAP in RPE1 and MCF7 cells, but only noticeably affects YAP in HEK293A cells when there is additional input from the Hippo pathway.

ER Stress Is Involved in YAP Inactivation Induced by COPI Subunit Depletion. Next, we examined potential links between the COPI complex and MAP2K3 for YAP activity regulation. COPI dysfunctions due to germline mutations in ARCN1 or COPA genes have been shown to activate the ER stress pathway in human COPA syndrome (16, 26). In addition, a previous study showed that ER stress signaling can increase the level of YAP Ser127 phosphorylation through the induction of the GADD34/PPI complex (27). First, we found that the disruption of the COPI complex by ARCN1 or COPA knockdown promotes activating phosphorylation on MAP2K3 (Fig. 5*A*). Quantitative increases and mobility shifts of PERK, an ER stress sensor, were induced by ARCN1 or COPA knockdown, indicating the activation of the ER stress pathway (Fig. 5*B* and *SI Appendix*, Fig. S8*A*). The transcription of GADD34 and ATF4, which are up-regulated during the apoptotic phase of prolonged ER stress, also increased after ARCN1 or COPA knockdown (*SI Appendix*, Fig.

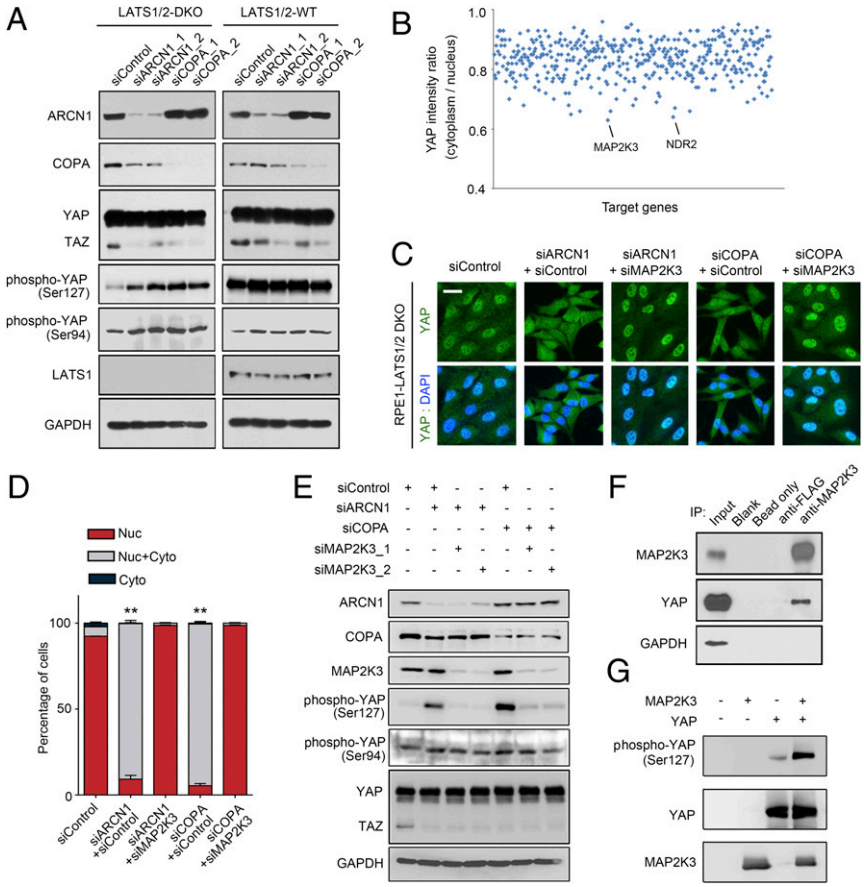

Fig. 4. MAP2K3 may mediate YAP Ser127 phosphorylation induced by COPI subunit depletion. (*A*) Immunoblot analysis of the indicated proteins. RPE1-LATS1/2 DKO and WT cells transfected with ARCN1 or COPA siRNAs were analyzed. (*B*) A graph showing the result of a kinome siRNA library screen. RPE1-LATS1/2 DKO cells were cotransfected with ARCN1 siRNA and human kinome siRNA library, and the mean cytoplasmic/nuclear ratio of YAP intensity was plotted. (*C*) Immunofluorescence micrographs showing YAP localization in RPE1-LATS1/2 DKO cells transfected with the indicated siRNAs for 48 h. (Scale bar, 20 μm.) (*D*) Quantification of the experiment presented in *C*. Error bars represent SEM ($n = 3$ independent experiments). $^{**}P < 0.01$ (*t* test). (*E*) Immunoblot analysis of the indicated proteins. RPE1-LATS1/2 DKO cells transfected with the indicated siRNA pairs were analyzed. (*F*) Immunoprecipitation analysis showing the interaction between endogenous MAP2K3 and YAP. (*G*) In vitro kinase assay showing YAP Ser127 phosphorylation by MAP2K3.

S8*B*). Pharmacologic induction of ER stress using thapsigargin or tunicamycin in RPE1-LATS1/2 DKO cells promoted MAP2K3 activation and YAP phosphorylation at Ser127 (Fig. 5*C*). Protein levels of GADD34 and phospho-P38 MAPK also increased after drug treatment (Fig. 5*C*). Analysis of publicly available microarray data (28) showed that tunicamycin treatment decreases the expression of YAP signature genes in mouse liver tissues (Fig. 5*D*). Prolonged ER stress is known to induce apoptosis by activating ASK1 (also called MAP3K5), and ASK1 induces P38 signaling through activation of downstream MAP kinase kinases, including MAP2K3 (29, 30). Thus, we tested the involvement of ASK1 in the regulation of YAP. Depletion of COPA promoted activating ASK1 phosphorylation, and ASK1 coknockdown reversed the increased MAP2K3 and YAP phosphorylation (Fig. 5*E*). Moreover, tunicamycin treatment increased ASK1 phosphorylation, and depletion of ASK1 reversed YAP Ser127 phosphorylation induced by tunicamycin (Fig. 5*F*). MAP2K3 or ASK1 knockdown blocked ER stress-mediated cytoplasmic retention of YAP in LATS1/2-DKO cells (Fig. 5*G*). These results together suggest that ER stress signaling is involved in the regulation of YAP activity through the COPI-MAP2K3 pathway.

We next tested whether P38 is involved in YAP regulation by MAP2K3 in the LATS1/2 DKO context. Treatment of cells with the P38 inhibitor SB203580 did not affect the YAP cytoplasmic sequestration due to ARCN1 and COPA knockdown (*SI Appendix*, Fig. S9*A*). In addition, SB203580 treatment did not show a notable influence on the level of YAP Ser127 phosphorylation (*SI Appendix*, Fig. S9*B*). Elevation of P38 phosphorylation after SB203580 treatment is likely to be ascribed by release of the negative feedback regulation of P38 phosphorylation. P38 has been reported to sequester TEADs to the cytoplasm to repress the YAP-TEAD activity (31). However, TEAD cytoplasmic sequestration was not observed in cells depleted of COPI subunits and MAP2K3 (*SI Appendix*, Fig. S9*C*). AMPK has been shown to directly phosphorylate YAP in a Hippo-independent manner and is also involved in the modulation of the ER stress pathway (9, 32). We observed an elevation of phospho-AMPK levels after ARCN1 or COPA knockdown (*SI Appendix*, Fig. S10*A*). In addition, COPI depletion-mediated Ser94 phosphorylation was reversed by treatment of the AMPK inhibitor dorsomorphin in LATS-DKO RPE1 cells (*SI Appendix*, Fig. S10*B*). However, dorsomorphin treatment did not significantly decrease YAP Ser127 phosphorylation. These results support the idea that MAP2K3 is responsible mainly for the phosphorylation of YAP Ser127 in LATS1/2 DKO cells.

Inhibition of COPA or YAP Promotes the Expression of PTGS2 and Proinflammatory Cytokines. COPA syndrome is characterized by inflammation and immune dysregulation that appear in childhood in multiple systems of the body, including the lungs (16). To investigate the effect of COPA depletion on the lung

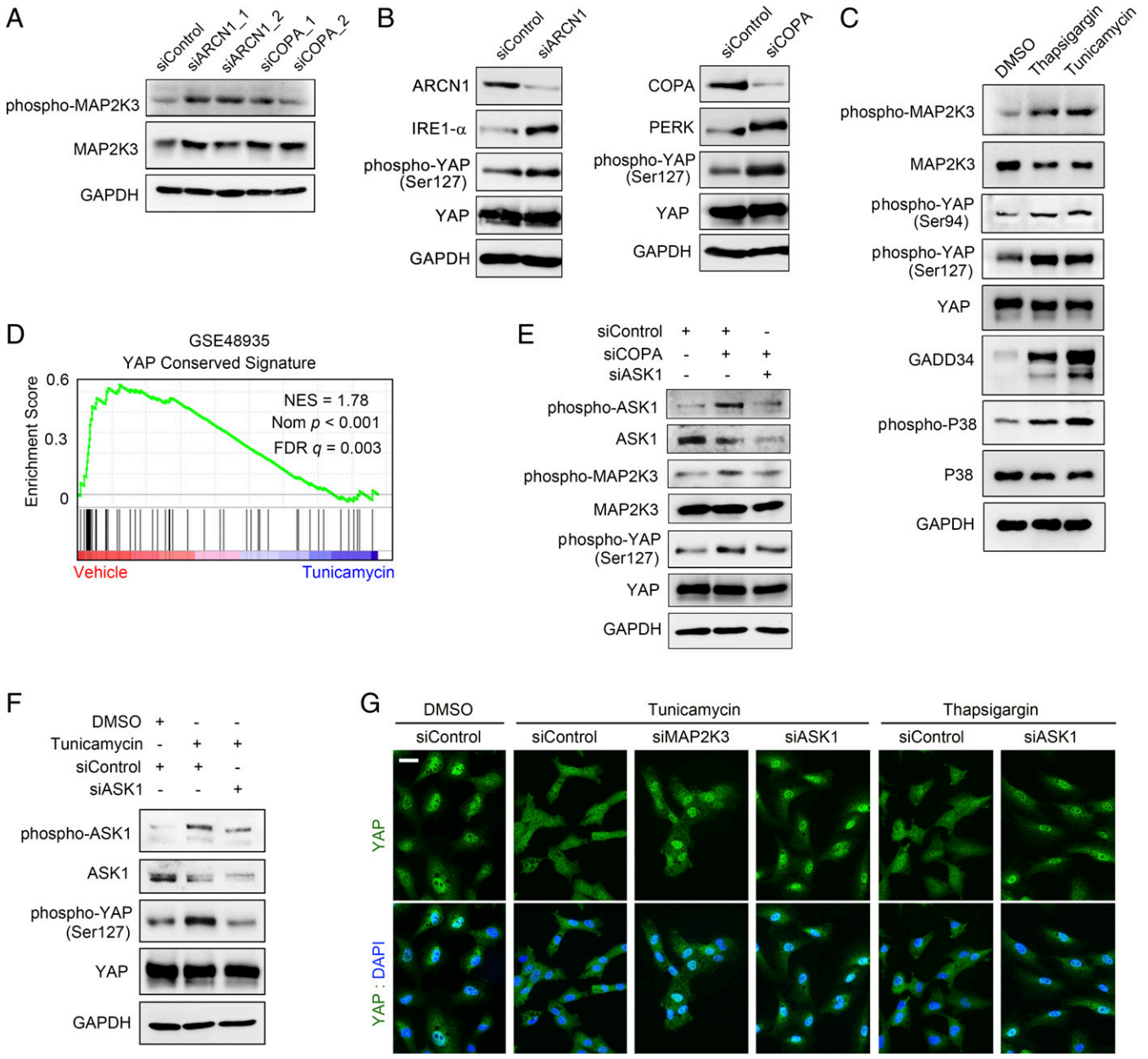

Fig. 5. COPI disturbances can inhibit YAP through the induction of persistent ER stress. (*A*) Immunoblot analysis of MAP2K3 phosphorylation in ARCN1 or COPA-depleted RPE1-LATS1/2 DKO cells. (*B*) Immunoblot analysis of ER stress markers in RPE1-LATS1/2 DKO cells transfected with the indicated siRNAs. (*C*) Immunoblot analysis of the indicated proteins in RPE1-LATS1/2 DKO cells treated with the indicated chemicals for 12 h. (*D*) GSEA analysis of published microarray data (GSE48935) demonstrating a down-regulation of YAP signature genes in liver tissue of C57B6 mice after intraperitoneal injection of tunicamycin. (*E*) Immunoblot analysis of the indicated proteins. RPE1-LATS1/2 DKO cells transfected with the indicated siRNA pairs were analyzed. (*F*) Immunoblot analysis of the indicated proteins in RPE1-LATS1/2 DKO cells. Cells were transfected with the siRNAs for 72 h and the chemicals were added 18 h before lysis. (*G*) Immunofluorescence micrographs showing YAP localization in RPE1-LATS1/2 DKO cells treated with the indicated siRNAs and chemicals. (Scale bar, 20 μm.)

epithelium, we performed liposome-based siRNA delivery to mouse airways at postnatal day 8 by intranasal inhalation (33, 34). Enhanced green fluorescent protein plasmid (pEGFP) vector was introduced along with siRNAs to mark the region where siRNAs were delivered. EGFP fluorescence was observed in some regions of bronchi and bronchioles 3 d after the administration of siRNA/pEGFP-loaded liposomes. We focused on $EGFP^+$ bronchioles with a diameter of 50 to 100 μm. Reduction of Copa protein levels after Copa siRNA transfection in cultured mouse cells and $EGFP^+$ mouse bronchioles was confirmed by immunoblot analysis and immunofluorescence staining, respectively (*SI Appendix*, Fig. S11 *A* and *B*). Administration of Copa siRNA/pEGFP-loaded liposomes increased the number of $F4/80^+$ macrophages around $EGFP^+$ bronchioles, indicating that Copa depletion induced lung inflammation (Fig. 6 *A* and *B*). No apparent nuclear enrichment of YAP in $EGFP^+$ bronchiole cells was observed in both control and Copa siRNA groups. A recent study showed that YAP and TAZ are required for the regeneration of damaged alveolar epithelium and the resolution of lung inflammation (35). To induce acute lung damage, cholera toxin was administered with siRNA/pEGFP-loaded liposomes. Under this condition, fractions of $EGFP^+$ bronchiole cells treated with control siRNA showed nuclear Yap

enrichment (Fig. 6*C*). Importantly, the percentage of cells exhibiting nuclear Yap enrichment was reduced by Copa siRNA transfection (Fig. 6 *C* and *D*). These results suggest that Yap activation for lung regeneration does not occur in Copa-deficient conditions.

ER stress signaling can induce inflammation through up-regulation of proinflammatory cytokines such as IL1B and IL6 (16, 36). Knockdown of ARCN1 resulted in up-regulation of proinflammatory cytokines and the potent inflammatory mediator *PTGS2* (also known as *COX2*) as well as the ER stress pathway molecules *HSPA5* and *ATF4* (*SI Appendix*, Fig. S12*A*). COPA depletion also induced the expression of proinflammatory cytokines (Fig. 6*E*). Moreover, the expression of proinflammatory cytokines was increased by YAP/TAZ knockdown (Fig. 6*E*), suggesting that YAP/TAZ inactivation contributes to proinflammatory cytokine production that occurs in response to COPI deficiencies. We revisited the gene expression data of our previous study (23) and found that, among the inflammatory genes up-regulated by ARCN1/COPA-depletion, *PTGS2* was consistently increased by knockdown of YAP/TAZ in melanoma cells (*SI Appendix*, Fig. S12*B*). We further examined the regulation of PTGS2 expression. Immunoblot analysis demonstrated up-regulation of PTGS2 protein levels in RPE1 and SKMEL28 cells after ARCN1 or COPA knockdown (*SI Appendix*, Fig. S12*C*). Depletion of YAP/TAZ increased PTGS2 messenger RNA (mRNA) and protein levels in RPE1, SKMEL28, and A549 cells (Fig. 6 *F* and *G*). By contrast, transfection of constitutively active YAP constructs decreased PTGS2 mRNA and protein levels (*SI Appendix*, Fig. S12 *D* and *E*) (37). These results indicate that PTGS2 expression is suppressed by YAP/TAZ activity. To test whether YAP acts as a repressor of PTGS2 transcription, we examined the PTGS2 promoter region. Six YAP/TEAD-binding sequences (CATTCC) (3) were located in the PTGS2 promoter (*SI Appendix*, Fig. S12*F*). The promoter sequence from −2 kb upstream to the transcription start site was inserted into a luciferase reporter vector (*SI Appendix*, Fig. S12*G*). PTGS2 promoter-driven reporter activity was significantly increased by YAP/TAZ knockdown (*SI Appendix*, Fig. S12*H*). Taken together, these results suggest that YAP inhibit proinflammatory gene expression and that YAP inactivation can exacerbate lung damage from COPA-related inflammation.

Discussion

Recent studies have reported important roles of YAP/TAZ in tumor stem-like properties, drug resistance, and lymph node or blood-borne metastasis in human cancers (2, 8, 12, 13, 38). Genetic or epigenetic silencing of core Hippo components has been identified across human cancers (12, 14). Effective and selective agents that activate Hippo kinases in cancer have not yet been developed. Thus, there have been research efforts to find Hippo-independent positive regulators of YAP/TAZ as a drug target whose inhibition can exert an anticancer effect. Gene silencing with specific siRNAs has facilitated genome-level phenotypic analysis. In the present study, we performed a genome-wide RNAi screen to systematically search for novel Hippo-independent YAP regulators. We found that interruption of the COPI vesicle-trafficking pathway can attenuate the activity of YAP/TAZ through the function of MAP2K3, a dual specific kinase activated by environmental stress. Our study also suggests that there are a number of kinases that can provide regulatory inputs to YAP in response to cellular stresses in the absence of LATS1/2 (Fig. 4*B*).

COPI subunits are constitutive housekeeping genes that play an essential role in membrane-related cellular functions, including vesicle transport and nuclear envelope maintenance. Thus, it is surprising that COPI addiction is induced by oncogenic KRAS together with loss of LKB1 or AMPK in non–small-cell-lung-cancer cell lines (39). We found that the COPI complex is required for maintaining high levels of EGFR and c-MYC in vemurafenib-resistant melanoma cells in which YAP is activated. Moreover, multiple YAP-dependent cancer cells showed a high dependence on intact COPI function for survival. Upon energy stress, LKB1-AMPK inhibits YAP activity by phosphorylating Ser94 residue (9). We speculate that YAP addiction is associated with COPI addiction in cancers exhibiting loss of LKB1/AMPK activity. Our study provides a series of evidence suggesting that ER stress is involved in YAP inactivation due to COPI function disturbances. First, COPI subunit depletion resulted in up-regulation of several ER stress markers. Second, pharmacologic induction of ER stress, as well as COPI subunit depletion, promoted activating MAP2K3 phosphorylation and YAP Ser127 phosphorylation. Third, depletion of MAP2K3 or ASK1 prevented ER stress-induced YAP Ser127 phosphorylation. In addition, depletion of MAP2K3 or ASK1 reversed ER stress-mediated cytoplasmic sequestration of YAP. Based on these results we propose the following mechanism: COPI disturbance → prolonged ER stress → ASK1 activation → MAP2K3 activation → YAP inactivation. This inhibitory mechanism may be important to prevent YAP from interfering with the process by which persistent and severe ER stress induces cell death.

Although our study demonstrates the therapeutic utility of targeting ARCN1 or COPA in YAP-dependent cancer cells, it should be noted that the ER stress response pathway is also known to promote cancer development (40). Thus, it is important to find cancer types in which COPI inhibition has an optimal anticancer effect. Developing chemical inhibitors specific for the COPI complex would be also critical.

ER stress is a major contributor to inflammatory human diseases, such as rheumatoid arthritis and nonalcoholic fatty liver disease (41–43). Inflammatory arthritis and interstitial lung disease in COPA syndrome are also associated with ER stress (16). In this study, we show that persistent inflammation and lung damage from COPA-related ER stress are likely to be promoted by YAP inactivation and consequent PTGS2 up-regulation. PTGS2 is a therapeutic target of nonsteroidal antiinflammatory drugs, which are widely used in the clinic to inhibit the inflammatory process (44). Further research is needed to understand the specific role of YAP inactivation and PTGS2 up-regulation in COPA syndrome and other inflammatory diseases. In conclusion, this study provides a regulatory link between COPI, ER stress, and YAP.

Materials and Methods

For detailed materials and methods, see *SI Appendix*.

Cell Culture and siRNA Transfection. Human RPE1, MCF7, SKMEL28, HEK293T, and A549 cells and mouse IMCD3 cells were acquired from the American Type Culture Collection. MSTO-211H, 92.1, H2373, and OCM1 cells were a gift from Hyun Woo Park, Yonsei University, Seoul. LATS1/2 DKO HEK293A cells established by the laboratory of Kun-Liang Guan, University of California, San Diego, were acquired through Hyun Woo Park. Large frozen cell stocks were created to prevent contamination by other cell lines. All cell lines were used within 10 passages after being revived from the frozen stocks. Cells were free of *Mycoplasma* contamination as determined by staining cells with DAPI every two or three passages. siRNA transfection was performed with Lipofectamine RNAiMAX (Invitrogen) according to the manufacturer's instructions. AllStars Negative Control siRNA (Qiagen) was used as a control siRNA. The sequence of siRNAs used in this study is provided in *SI Appendix*, Table S1.

Genome-Wide siRNA Screen. A human whole-genome siRNA library (ON-TARGETplus, Dharmacon) was used in this study. Four different siRNAs targeting 18,055 human genes were spotted as a pool on 384-well plates (CELLSTAR, Greiner) using the BioMEK FX Laboratory Automation Workstation (Beckman Coulter). Anti-YAP immunofluorescence images were acquired using the Opera QEHS confocal microscope (Perkin-Elmer) and were transferred to the Columbus Database (Perkin-Elmer) for storage and further analysis. Nuclear and cytoplasmic YAP immunofluorescence intensity were analyzed by CellProfiler software (Broad Institute).

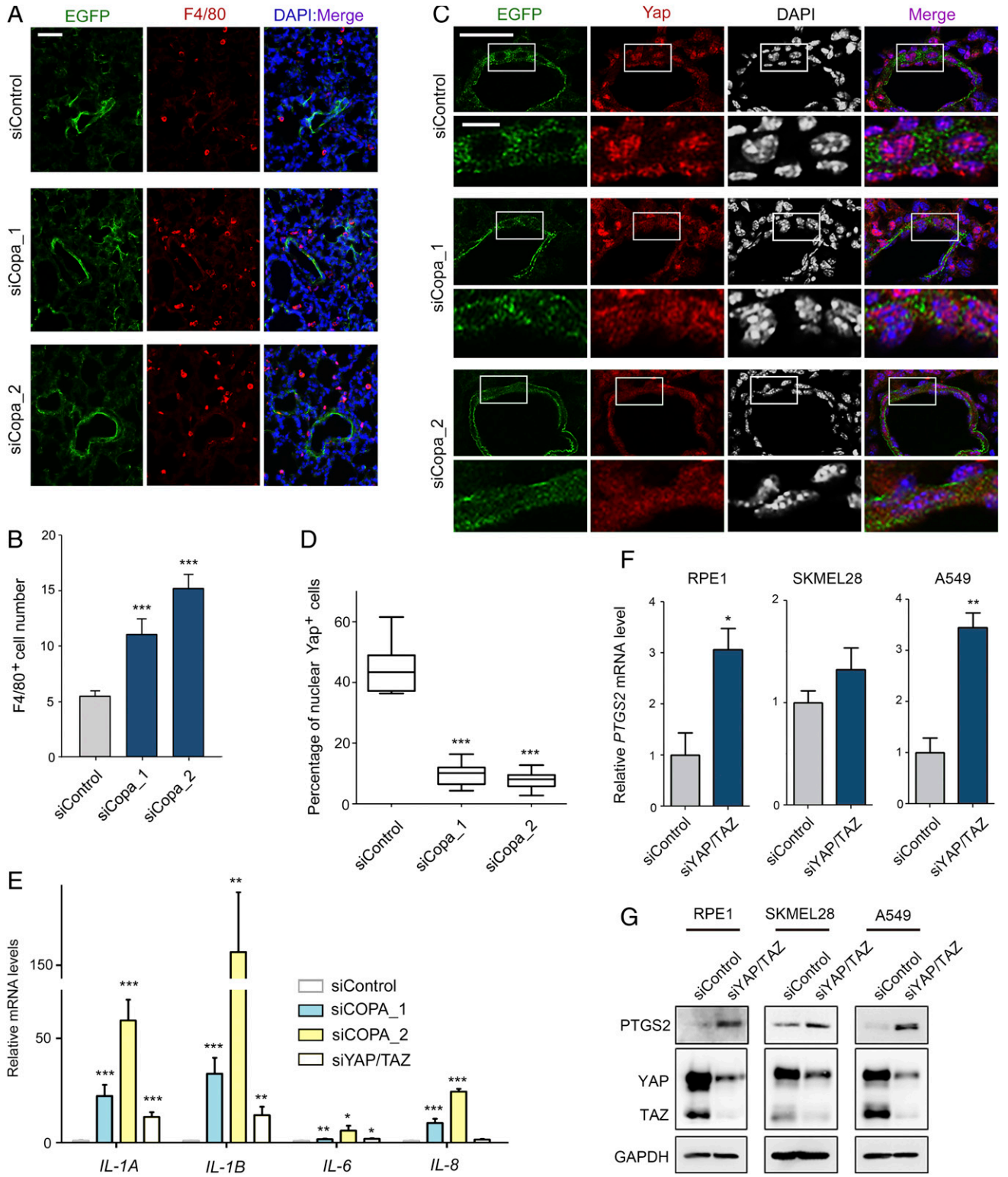

Fig. 6. Inflammation of the mouse bronchial epithelium due to Copa knockdown is accompanied by Yap inactivation, which can cause PTGS2 up-regulation. (*A*) Liposomes loaded with siRNA and pEGFP were delivered to the neonatal mouse lungs by intranasal inhalation. After 3 d, the inflammatory response was evaluated based on the increase in the number of macrophages labeled with anti-F4/80 antibody. (*B*) Quantification of the experiment presented in *A*. F4/80$^+$ cells in the 0.12-mm^2 area around EGFP$^+$ bronchioles were counted. Error bars represent SEM (n = 14 independent fields from two mice per group). (*C*) Cholera toxin was administered with siRNA/pEGFP-loaded liposomes. After 3 d, Yap activity was evaluated by immunofluorescence staining. (*D*) Quantification of the experiment presented in *C* (n = 20 bronchiole sections from four mice per group). (*E*) qRT-PCR analysis of the expression of proinflammatory cytokines in PRE1 cells after transfection with the indicated siRNAs for 48 h. (*F*) qRT-PCR analysis of the expression of *PTGS2* in the indicated cell lines after cotransfection with YAP and TAZ siRNAs. (*G*) Immunoblot analysis for the expression of the indicated proteins. Error bars in *E* and *F* represent SEM (n = 3 independent experiments). *$P < 0.05$, **$P < 0.01$, and ***$P < 0.001$ (t test). (Scale bars: 50 μm [*A* and *C*, *Top*] and 10 μm [*C*, second panel].)

Intranasal Delivery of siRNA-Loaded Liposomes. The animal care and experimental procedures used in this study were approved by the Institutional Animal Care and Use Committee at the Korea Advanced Institute of Science and Technology (KA2019-26). Invivofectaime 3.0 (Thermofisher) and lipofectamine 3000 (Thermofisher) were complexed with siRNA and pEGFP plasmid, respectively, according to the manufacturer's instruction. Liposomes loaded with siRNA and pEGFP were mixed together before delivery. Female CD-1 mice with neonates were purchased from OrientBio in Korea, and neonates were used for the experiment at postnatal day 8. Under mild anesthesia by isoflurane inhalation, the head of the mouse was manually restrained, and droplets of the liposome-formulated siRNA/pEGFP mixture were slowly administered to the nostril (1 μg siRNA and 0.2 μg plasmid in 5 μL of volume per mouse). At 72 h post administration, the mice were euthanized and lung sections were prepared.

Quantification and Statistical Analysis. Quantification of YAP localization in immunofluorescence images was performed by inspecting at least 150 to 200 cells stained with anti-YAP immunofluorescence. Confluence and cell clumps were avoided in quantification. YAP localization in immunofluorescence images was classified into three categories: nuclear (higher nuclear intensity than cytoplasmic intensity), nucleocytoplasmic (equal intensity of nucleus and cytoplasm), and cytoplasmic (higher cytoplasmic intensity than nuclear intensity). Data analysis was performed using GraphPad Prism version 6. For quantification of immunostaining in the mouse lung section, 7 to 10 images (200×) per mouse and 2 to 4 mice per condition were analyzed. All tests were two-tailed *t* test, and $P < 0.05$ was considered to indicate statistical significance.

Data Availability. All data are included in the paper and Datasets S1–S3.

ACKNOWLEDGMENTS. This study was supported by a National Research Foundation of Korea grant funded by the Korean Ministry of Science, Information and Communication Technology (2015M3A9B6027820 and 2020R1A2C3007748 to J.K. and 2018R1A2A3074597 and 2018R1A4A1024506 to J.E.L.) and by the Korea Basic Science Institute research program (T39730 to G.-H.K.). J.K. was supported by the LG Yonam Foundation of Korea.

1. A. Totaro, T. Panciera, S. Piccolo, YAP/TAZ upstream signals and downstream responses. *Nat. Cell Biol.* **20**, 888–899 (2018).
2. B. Zhao, K. Tumaneng, K. L. Guan, The Hippo pathway in organ size control, tissue regeneration and stem cell self-renewal. *Nat. Cell Biol.* **13**, 877–883 (2011).
3. M. Kim, T. Kim, R. L. Johnson, D. S. Lim, Transcriptional co-repressor function of the hippo pathway transducers YAP and TAZ. *Cell Rep.* **11**, 270–282 (2015).
4. Y. Gao *et al*., YAP inhibits squamous transdifferentiation of Lkb1-deficient lung adenocarcinoma through ZEB2-dependent DNp63 repression. *Nat. Commun.* **5**, 4629 (2014).
5. S. Dupont *et al*., Role of YAP/TAZ in mechanotransduction. *Nature* **474**, 179–183 (2011).
6. F. X. Yu *et al*., Regulation of the Hippo-YAP pathway by G-protein-coupled receptor signaling. *Cell* **150**, 780–791 (2012).
7. J. Huang, S. Wu, J. Barrera, K. Matthews, D. Pan, The Hippo signaling pathway coordinately regulates cell proliferation and apoptosis by inactivating Yorkie, the Drosophila Homolog of YAP. *Cell* **122**, 421–434 (2005).
8. G. Halder, S. Dupont, S. Piccolo, Transduction of mechanical and cytoskeletal cues by YAP and TAZ. *Nat. Rev. Mol. Cell Biol.* **13**, 591–600 (2012).
9. J. S. Mo *et al*., Cellular energy stress induces AMPK-mediated regulation of YAP and the Hippo pathway. *Nat. Cell Biol.* **17**, 500–510 (2015).
10. S. Basu, N. F. Totty, M. S. Irwin, M. Sudol, J. Downward, Akt phosphorylates the Yes-associated protein, YAP, to induce interaction with 14-3-3 and attenuation of p73-mediated apoptosis. *Mol. Cell* **11**, 11–23 (2003).
11. S. W. Chan *et al*., Hippo pathway-independent restriction of TAZ and YAP by angiomotin. *J. Biol. Chem.* **286**, 7018–7026 (2011).
12. F. Zanconato, M. Cordenonsi, S. Piccolo, YAP/TAZ at the roots of cancer. *Cancer Cell* **29**, 783–803 (2016).
13. M. H. Kim, J. Kim, Role of YAP/TAZ transcriptional regulators in resistance to anticancer therapies. *Cell. Mol. Life Sci.* **74**, 1457–1474 (2017).
14. Y Wang *et al*., Comprehensive molecular characterization of the hippo signaling pathway in cancer. *Cell Rep.* **25**, 1304–1317.e5 (2018).
15. T. Moroishi, C. G. Hansen, K. L. Guan, The emerging roles of YAP and TAZ in cancer. *Nat. Rev. Cancer* **15**, 73–79 (2015).
16. L. B. Watkin *et al*.; Baylor-Hopkins Center for Mendelian Genomics, COPA mutations impair ER-Golgi transport and cause hereditary autoimmune-mediated lung disease and arthritis. *Nat. Genet.* **47**, 654–660 (2015).
17. F. A. Ran *et al*., Genome engineering using the CRISPR-Cas9 system. *Nat. Protoc.* **8**, 2281–2308 (2013).
18. G. Sorrentino *et al*., Metabolic control of YAP and TAZ by the mevalonate pathway. *Nat. Cell Biol.* **16**, 357–366 (2014).
19. J. Kim *et al*., Actin remodelling factors control ciliogenesis by regulating YAP/TAZ activity and vesicle trafficking. *Nat. Commun.* **6**, 6781 (2015).
20. B. Zhao *et al*., TEAD mediates YAP-dependent gene induction and growth control. *Genes Dev.* **22**, 1962–1971 (2008).
21. V. W. Hsu, S. Y. Lee, J. S. Yang, The evolving understanding of COPI vesicle formation. *Nat. Rev. Mol. Cell Biol.* **10**, 360–364 (2009).
22. J. B. Miesfeld *et al*., Yap and Taz regulate retinal pigment epithelial cell fate. *Development* **142**, 3021–3032 (2015).
23. M. H. Kim *et al*., Actin remodeling confers BRAF inhibitor resistance to melanoma cells through YAP/TAZ activation. *EMBO J.* **35**, 462–478 (2016).
24. B. Zhao, L. Li, K. Tumaneng, C. Y. Wang, K. L. Guan, A coordinated phosphorylation by Lats and CK1 regulates YAP stability through SCF(beta-TRCP). *Genes Dev.* **24**, 72–85 (2010).
25. L. Zhang *et al*., NDR functions as a physiological YAP1 kinase in the intestinal epithelium. *Curr. Biol.* **25**, 296–305 (2015).
26. K. Izumi *et al*., ARCN1 mutations cause a recognizable craniofacial syndrome due to COPI-mediated transport defects. *Am. J. Hum. Genet.* **99**, 451–459 (2016).
27. H. Wu *et al*., Integration of Hippo signalling and the unfolded protein response to restrain liver overgrowth and tumorigenesis. *Nat. Commun.* **6**, 6239 (2015).
28. A. M. Arensdorf, D. Dezwaan McCabe, R. J. Kaufman, D. T. Rutkowski, Temporal clustering of gene expression links the metabolic transcription factor HNF4α to the ER stress-dependent gene regulatory network. *Front. Genet.* **4**, 188 (2013).
29. H. Nishitoh *et al*., ASK1 is essential for endoplasmic reticulum stress-induced neuronal cell death triggered by expanded polyglutamine repeats. *Genes Dev.* **16**, 1345–1355 (2002).
30. H. Ichijo *et al*., Induction of apoptosis by ASK1, a mammalian MAPKKK that activates SAPK/JNK and p38 signaling pathways. *Science* **275**, 90–94 (1997).
31. K. C. Lin *et al*., Regulation of Hippo pathway transcription factor TEAD by p38 MAPK-induced cytoplasmic translocation. *Nat. Cell Biol.* **19**, 996–1002 (2017).
32. G. P. Meares *et al*., IRE1-dependent activation of AMPK in response to nitric oxide. *Mol. Cell. Biol.* **31**, 4286–4297 (2011).
33. L. A. Santry *et al*., AAV vector distribution in the mouse respiratory tract following four different methods of administration. *BMC Biotechnol.* **17**, 43 (2017).
34. Y. Huang *et al*., Pharmacokinetic behaviors of intravenously administered siRNA in glandular tissues. *Theranostics* **6**, 1528–1541 (2016).
35. R. LaCanna *et al*., Yap/Taz regulate alveolar regeneration and resolution of lung inflammation. *J. Clin. Invest.* **129**, 2107–2122 (2019).
36. A. M. Keestra-Gounder *et al*., NOD1 and NOD2 signalling links ER stress with inflammation. *Nature* **532**, 394–397 (2016).
37. J. M. Lamar *et al*., The Hippo pathway target, YAP, promotes metastasis through its TEAD-interaction domain. *Proc. Natl. Acad. Sci. U.S.A.* **109**, E2441–E2450 (2012).
38. C. K. Lee *et al*., Tumor metastasis to lymph nodes requires YAP-dependent metabolic adaptation. *Science* **363**, 644–649 (2019).
39. H. S. Kim *et al*., Systematic identification of molecular subtype-selective vulnerabilities in non-small-cell lung cancer. *Cell* **155**, 552–566 (2013).
40. J. R. Cubillos-Ruiz, S. E. Bettigole, L. H. Glimcher, Tumorigenic and immunosuppressive effects of endoplasmic reticulum stress in cancer. *Cell* **168**, 692–706 (2017).
41. S. A. Yoo *et al*., A novel pathogenic role of the ER chaperone GRP78/BiP in rheumatoid arthritis. *J. Exp. Med.* **209**, 871–886 (2012).
42. B. Porteiro *et al*., Hepatic p63 regulates steatosis via IKKβ/ER stress. *Nat. Commun.* **8**, 15111 (2017).
43. C. Lebeaupin *et al*., Endoplasmic reticulum stress signalling and the pathogenesis of non-alcoholic fatty liver disease. *J. Hepatol.* **69**, 927–947 (2018).
44. J. C. Frölich, A classification of NSAIDs according to the relative inhibition of cyclooxygenase isoenzymes. *Trends Pharmacol. Sci.* **18**, 30–34 (1997).